Evolution of dendrite morphology of a binary alloy under an applied electric current: An *in situ* observation

Tongmin Wang,[1,*] Jingjing Xu,[1] Tiqiao Xiao,[2] Honglan Xie,[2] Jun Li,[1] Tingju Li,[1] and Zhiqiang Cao[1]
[1]*School of Materials Science and Engineering, Dalian University of Technology, Dalian 116023, China*
[2]*Shanghai Synchrotron Radiation Facility, Shanghai Institute of Applied Physics, Shanghai 215600, China*
(Received 1 October 2009; revised manuscript received 2 April 2010; published 29 April 2010)

Synchrotron radiation imaging technique was used to *in situ* observe the dendrite growth of a solidifying Sn-Bi binary alloy under a direct current (dc) electric field. By applying a dc (7–32 A/cm^2), the dendrite branching was suppressed, the dendrite tip was modified to be round or flat, and no tertiary dendrite was found. With increasing dc density, the dendrite morphology was changed from *columnar dendritic* to *equiaxed cellular* to *equiaxed dendritic*. In particular, the primary dendrite branched following a tip-split manner in a higher intensity dc. The influence of dc on the evolution of dendrite morphology was discussed.

DOI: 10.1103/PhysRevE.81.042601 PACS number(s): 68.70.+w, 07.85.Qe, 81.30.Fb

The application of electric current during metal solidification process has been tried since 1960s, and it was found that the electric current can modify the process of nucleation and evolution of microstructure. Primary goal of those studies was for the grain refinement by applying dc [1–3], alternating current (ac) [4], electric current pulse (ECP) [5–7]. Significant refinement efficiency on eutectic or noneutectic microstructure has been achieved by an applied electric current for low melting Sn-Pb (Bi) alloy, middle melting Al-Cu alloy, even for high melting steel and iron. It is well known that an electric current usually impacts on a solidifying melt through a series of effects: electromigration, electricity-to-heat, electromagnetic force, etc. Based on these effects, a number of various refining mechanisms have been established: for example, the improvement of interface stability and the specialty of current crowding [2], the change of solute diffusion and the selectivity of electric current [4], the breaking off dendrite arm [5], the enhancement of nucleation rate [6,7], etc. Nevertheless, each of them is hard to be fully confirmed. Sometimes, confliction occurs to each other among them for explaining a same phenomenon. Influence mechanism of electric current on solidifying alloy is still controversial.

A confirmed fact is, however, all the studies mentioned above were done by analyzing microstructure/macrostructure after complete solidification or interrupting solidification by quenching. As a result, the evolution of grain morphology during solidification cannot be *in situ* observed. To better understand the behavior of grain growth under dc, an *in situ* imaging technique with intense, coherent and monochromatic synchrotron x ray was used in this work. Although this technique has been applied for the real-time study on growing dendrites of metallic alloys [8–12], no study on the effect of electric current was reported.

In this paper, we focused on observing the evolution of dendrite morphology of a solidifying Sn-Bi alloy under an applied dc field, and finding the interesting dynamic phenomena which have not been revealed by the traditional approaches. On the basis of real-time observations, we try to understand how dc works on the dendrite growth in a solidifying melt.

A binary alloy with a composition of Sn-12 wt %Bi was prepared. The behavior of dendrite growth can be directly observed due to the x-ray absorption difference between Sn and Bi. The high temporal and spatial resolutions enough for clear and fast imaging can be achieved by using a synchrotron x ray. A well polished thin alloy sample with a thickness of 100 μm was cut into a rectangular slice of 1.0×2.0 cm^2, and then sandwiched between two 1-mm-thick quartz glass plates. A 60 μm thick polytetrafluoroethylene (PTFE) sheet was also placed between the two quartz glass plates, and used to fix the alloy sample. Clips pinched the two glass plates to keep the alloy sample still during solidification. Figure 1 shows the schematic diagram of experimental setup. As shown in Fig. 1, the dc was imposed to the alloy by connecting the sample to a dc generator. Two pieces aluminum foils acted as the positive electrode (upside) and negative one (downside), respectively. A special electric furnace was designed for melting the alloy sample during the synchrotron microradiography experiment. A cooling rate can be controlled by thyristor temperature controller. There is a window in the middle of furnace for x ray passing through the sample. A charge-coupled device (CCD) camera is set behind the furnace to dynamically acquire the time-sequenced images.

The imaging experiments were carried out at the beamline BL13W1 of Shanghai Synchrotron Radiation Facility

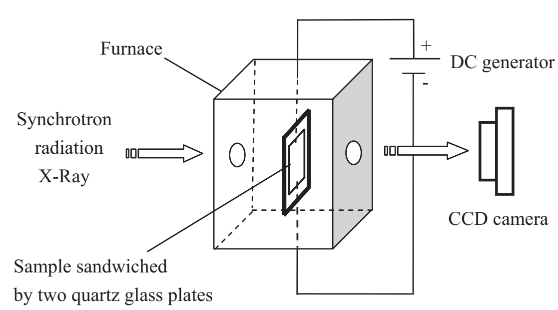

FIG. 1. Schematic of synchrotron radiation imaging experiment.

*Corresponding author. FAX: +86 411 84706790; tmwang@dlut.edu.cn

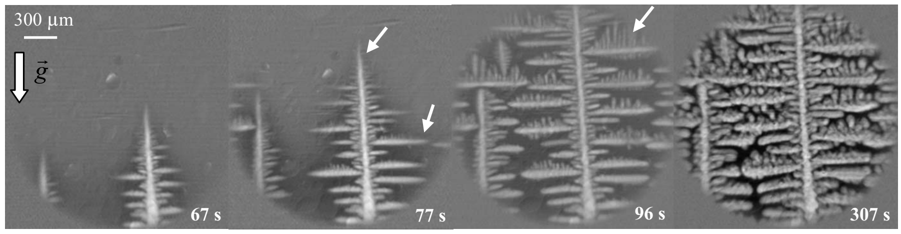

(a) Without DC. *Columnar dendritic* grains; thin primary, secondary and tertiary dendrite arms with sharp tips (denoted by arrows).

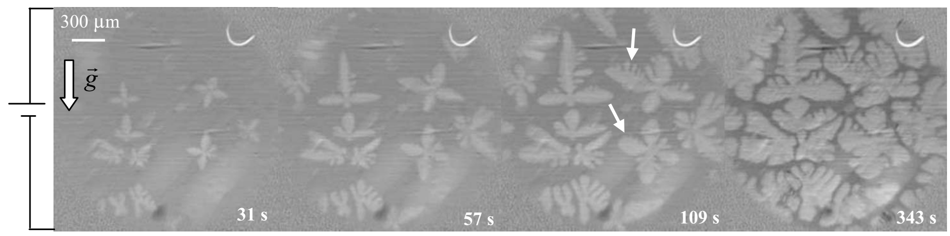

(b) DC density: 7 A/cm^2. *Equiaxed cellular* grains; thick primary arms, degenerate secondary arms with round tips (denoted by arrows); no tertiary dendrite branching.

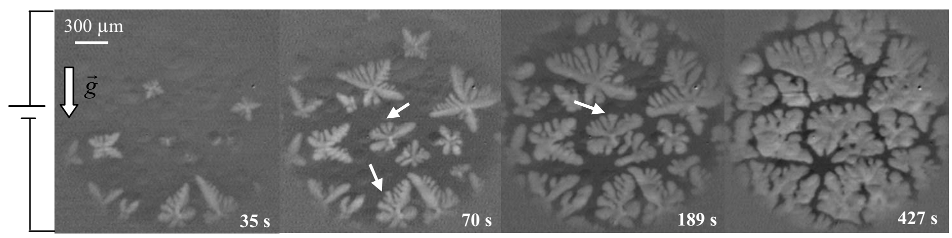

(c) DC density: 19 A/cm^2. *Equiaxed dendritic* grains; some primary dendrite tips split for branching (denoted by arrows); no tertiary dendrite branching.

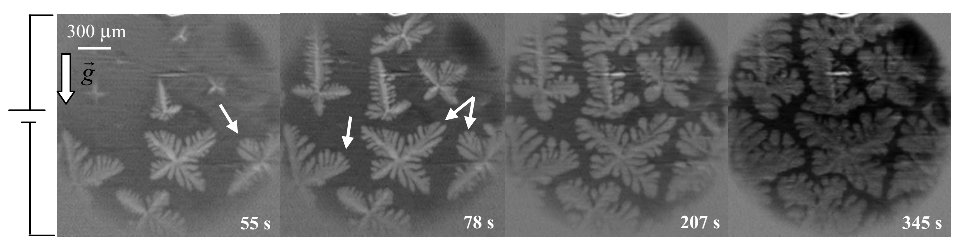

(d) DC density: 32 A/cm^2. *Equiaxed dendritic* grains; some primary dendrite tips split for branching (denoted by arrows); no tertiary dendrite branching.

FIG. 2. *In situ* observations on the dendritic growth of a solidifying Sn-12 wt %Bi alloy under dc field. Cooling rate is 1.5 k/min.

(SSRF), a third generation synchrotron radiation facility in China. The details of the imaging experiments without considering the effect of electric current has been reported in our previous papers [13,14]. Only a brief introduction is presented here. The CCD camera has a circle view of 750 pixels in diameter. The pixel size is down to 2.25 μm and the exposure time of per frame is 2–4 s, which are sufficient for clearly catching the evolution of dendrite morphology. In present experiments, the energy of monochromatic beam was 20 keV. The sample-to-detector distance was 15 cm. The alloy was melted completely with a superheat of 8 K, and then cooled at a cooling rate of 1.5 K/min. A little gradient might exist in the vertical direction of sample due to the internal construction of furnace, but it is hard to be measured quantitatively. Four experiments were made: one case is the solidification without dc; others are with various electric current densities of 7, 19, and 32 A/cm^2, respectively. dc was applied to the entire solidification process.

Figure 2 shows the evolutions of grains' morphology of different experiments. Without dc, the grains grew in a columnar manner due to a little temperature gradient in the vertical direction, as shown in Fig. 2(a). Very thin primary, secondary, tertiary dendrite arms and sharp dendrite tips were also found. The *columnar dendritic* grains grew fast and finally reached a large size of around 2 mm.

Once a dc density of 7 A/cm^2 was imposed, the dendrite branching and arm growth were significantly restrained as shown in Fig. 2(b). The primary arms grew to be thick, and the secondary arms were suppressed to be degenerate. Both the primary and secondary arm tips tended to be round or even flat. The sharp tips and tertiary dendrites were hardly found. The grains tended to be an *equiaxed cellular* morphology.

With increasing dc density ($\sim$19 A/cm^2, $\sim$32 A/cm^2), as shown in Figs. 2(c) and 2(d), some primary arm tips tended to split and form concave pits. Several secondary

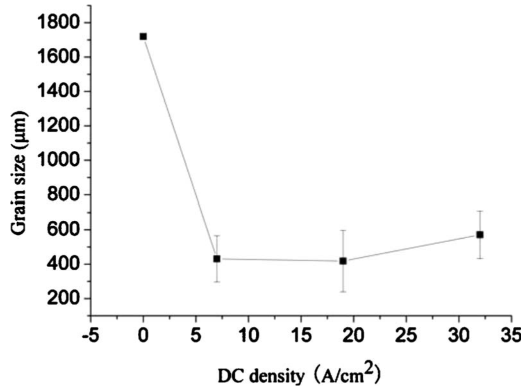

FIG. 3. Variation in mean grain size with dc density (error bar represents standard deviation).

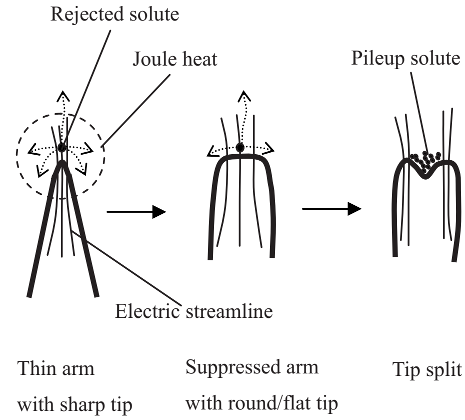

FIG. 4. Schematic explanation to the influence of dc on the evolution of dendrite morphology.

dendrites started to branch obliquely, whose directions are no longer perpendicular to their parent-primary arms as normal. Eventually a nearly *equiaxed dendritic* morphology was formed.

Figure 3 shows the mean grain size together with standard deviation varying with dc density. Each grain within a circle view of Figs. 2(a)–2(d) was measured, respectively. The mean grain size was obtained by averaging all the grains within the circle view. The grain size turned a sudden decrement when a dc density of 7 A/cm^2 was imposed. It is due to the significant suppression of dc on dendritic growth. With increasing dc density from 19 to 32 A/cm^2, the grain size was first decreased and then increased slightly. It might be a result of the tip-split of primary dendrite arm, or a fluctuation of solute, free energy and chemical potential, or something else due to dc field? Since the superthin alloy sample ($\sim$100 μm) in our experiments was pinched by two quartz glass plates tightly, any flow driven by thermosolutal field or dc field could be dragged to some extent by the viscosity forces of quartz glass walls. Therefore, the flow effect might be considered as less importance. The *in situ* observations give a proof that grain size is not always decreased with increasing current density but limited in the range below a critical current density.

An explanation to the influence mechanism of dc on the evolution of dendrite morphology was schematically illustrated in Fig. 4 based on our *in situ* observations and the previous work by other researchers [2,4]. Since the electrical conductivity of solid Sn-12 wt %Bi alloy is much bigger than that of liquid alloy, the electric streamlines prefer passing through solid to liquid. They easily gather in a sharp tip of dendrite to generate much more heat there due to both the Joule heating effect and the current crowding effect. The heat causes a rising temperature around the sharp dendrite tip by which the tip growth can be significantly suppressed. Accordingly, the sharp tip tends to be round or even flat in a self-adaptive way to scatter the electric streamlines for reducing Joule heat in order to keep growing. Since dc brings Joule heat into the solidifying melt, the solidification time was found to be increased with increasing dc density, that is, the solidification velocity was decreased with increasing dc density.

Very thin tertiary dendrite can hardly be initiated under dc due to aforementioned reason. Only a few secondary dendrites can survive due to some fluctuations in solidification. The survived secondary dendrites are still restrained for further growing by dc. Eventually a degenerate morphology is formed. The phenomena can also be explained from a viewpoint of interface energy and stability [2,4,15,16]. The influence of dc on solid-liquid interface energy can be described by the equation [2]: $\sigma_{s-l}=\sigma_0+w\cdot I^2$, where σ_{s-l} and σ_0 are specific interface energies with and without current effect, and w is a coefficient related to the solute concentration and electric parameters of solid and liquid phases. It is clear that the interface energy is increased with increasing current density. Higher interface energy enhances the stability of the solid/liquid interface. Hence any fluctuation of interface (e.g., planar to cellular or cellular to dendritic. i.e., dendrite branching) will be suppressed.

However, with increasing electric current density, a special tip-split scenario occurred to the primary arm resulting in a "branching" of the primary dendrite. As illustrated in Fig. 4, the solute is rejected gradually to the front of a growing dendrite tip during solidification. It is more difficult for the rejected solute to transversely diffuse from the tip center toward its lateral sides in case of a round or flat (higher dc density case) tip rather than a sharp one. The pileup solute becomes an obstacle opposite to the tip growing by changing the constitutional undercooling, thus a concave pit is formed. The pit is expended with the continuous growing of tip and the segregation of solute. Meanwhile, a tip is split into two tips. The two new tips will attract the electric streamlines again due to the current crowding effect. The Joule heat produced by electric current will slow down the growing rate of tips. Therefore, the evolution of tip split is actually determined by both the pileup solute and the Joule heat. The tip split will be formed if the former brings stronger effect than the latter or disappeared on the contrary.

In summary, *in situ* observation results of the dendrite growth of a solidifying Sn-12 wt %Bi alloy under dc field were reported and tried for being understood. In our discussion, the effects of Joule heat, current crowding, interface energy and constitutional undercooling have been taken into account. Actually, other effects such as Peltier heat, electromigration, nucleation rate change, etc. might also play a not negligible role. Further studies including *in situ* investigation together with necessary modeling work are desired to quantitatively verify the proposed explanations. Nevertheless, this study opens a new window to *in situ* investigate the microstructure evolution of an optically opaque alloy during solidification under imposed external fields, such as electric field, magnetic field and supersonic field, etc.

The authors gratefully acknowledge the support of the National Natural Science Foundation of China (Grants No. 50601003 and No. 50971032), and New Century Excellent Talents in University (Grant No. NCET-07-0137). Many thanks are expressed to Professor Menghuai WU for a lot of corrections to this paper, as well for his insightful comments and suggestions. Thanks are also extended to Professor Mingfang ZHU, Professor Jiuzhou ZHAO, Dr. Gang SONG for correcting this paper, to Dr. Yajun TONG for assisting the synchrotron microradiography experiments.

[1] A. K. Misra, Metall. Trans. **16A**, 358 (1985).
[2] G. W. Chang, J. P. Yuan, Z. D. Wang, C. J. Wu, X. H. Wang, and H. Q. Hu, Trans. Nonferrous Met. Soc. China **10**, 611 (2000).
[3] H. Conrad, Mater. Sci. Eng., A **287**, 205 (2000).
[4] S. R. Coriell, G. B. McFadden, A. A. Wheeler, and D. T. J. Hurle, J. Cryst. Growth **94**, 334 (1989).
[5] M. Nakada, Y. Shiohara, and M. C. Flemings, ISIJ Int. **30**, 27 (1990).
[6] J. P. Barnak, A. F. Sprecher, and H. Conrad, Scr. Metall. Mater. **32**, 879 (1995).
[7] X. L. Liao, Q. J. Zhai, J. Luo, W. J. Chen, and Y. Y. Gong, Acta Mater. **55**, 3103 (2007).
[8] R. H. Mathiesen, L. Arnberg, F. Mo, T. Weitkamp, and A. Snigirev, Phys. Rev. Lett. **83**, 5062 (1999).
[9] D. Ruvalcaba, R. H. Mathiesen, D. G. Eskin, L. Arnberg, and L. Katgerman, Acta Mater. **55**, 4287 (2007).
[10] H. Yasuda, I. Ohnaka, K. Kawasaki, A. Sugiyama, T. Ohmichi, J. Iwane, and K. Umetani, J. Cryst. Growth **262**, 645 (2004).
[11] B. Li, H. D. Brody, and A. Kazimirov, Phys. Rev. E **70**, 062602 (2004).
[12] B. Billia, N. Bergeon, H. Nguyen Thi, H. Jamgotchian, J. Gastaldi, and G. Grange, Phys. Rev. Lett. **93**, 126105 (2004).
[13] T. M. Wang, J. J. Xu, W. X. Huang, J. Li, S. W. Cai, T. J. Li, and J. Z. Jin, in *Modeling of Casting, Welding, and Advanced Solidification Processes—XII*, edited by S. L. Cockcroft and D. M. Maijer (TMS, Pennsylvania, 2009), pp. 613–617.
[14] T. M. Wang, J. J. Xu, J. Li, W. X. Huang, S. C. Liu, T. J. Li, Sci. China, Ser. E: Technol. Sci. (to be published).
[15] W. W. Mullins and R. F. Sakerka, J. Appl. Phys. **35**, 444 (1964).
[16] W. Kurz and D. J. Fisher, *Fundamentals of Solidification* (Trans Tech Publications Ltd., Aedermannsdorf, 1992) reprinted version.